SIAM J. NUMER. ANAL.
Vol. 52, No. 5, pp. 2555–2573

SUPERCONVERGENCE OF DISCONTINUOUS GALERKIN METHODS FOR LINEAR HYPERBOLIC EQUATIONS*

WAIXIANG CAO†, ZHIMIN ZHANG‡, AND QINGSONG ZOU§

Abstract. In this paper, we study superconvergence properties of the discontinuous Galerkin (DG) method for one-dimensional linear hyperbolic equations when upwind fluxes are used. We prove, for any polynomial degree k, the $2k+1$th (or $2k+1/2$th) superconvergence rate of the DG approximation at the downwind points and for the domain average under quasi-uniform meshes and some suitable initial discretization. Moreover, we prove that the derivative approximation of the DG solution is superconvergent with a rate $k+1$ at all interior left Radau points. All theoretical findings are confirmed by numerical experiments.

Key words. discontinuous Galerkin method, superconvergence, hyperbolic, Radau points, cell average, initial discretization

AMS subject classifications. 65M15, 65M60, 65N30

DOI. 10.1137/130946873

1. Introduction.

Discontinuous Galerkin (DG) methods, originally developed for neutron transport problems [17], are a class of finite element methods (FEMs) using completely discontinuous piecewise polynomial space. Due to its flexibility for arbitrarily unstructured meshes, the efficiency in parallel implementation, and the ability to easily handle complex geometries or interfaces and accommodate arbitrary *h*-*p* adaptivity, the DG method has gained popularity in solving various differential equations and attracts intensive theoretical studies. We refer to [9, 10, 11, 12, 13, 14] and the references cited therein for an incomplete list of references.

In the past several decades, there also has been considerable interest in studying superconvergence properties of DG methods. We refer to [1, 2, 18, 21] for ordinary differential equations, [3, 4] for multidimensional first order hyperbolic systems, [7, 8] for one-dimensional hyperbolic conservation laws and time-dependent convection-diffusion equations, and [16] for one- and two-dimensional hyperbolic equations based on the Fourier approach. Very recently, Yang and Shu in [19] studied superconvergence properties of a DG method for linear hyperbolic equations when upwind fluxes were used. They proved a $k+2$th superconvergence rate of the DG approximation at the right Radau points and for the cell average under suitable initial discretization. They also presented numerically, for $k=1,2$, a $2k+1$th superconvergence rate of the DG solution at the downwind points and for the cell average. However, a theoretical proof

*Received by the editors November 27, 2013; accepted for publication (in revised form) August 19, 2014; published electronically October 21, 2014.
http://www.siam.org/journals/sinum/52-5/94687.html
†Beijing Computational Science Research Center, Beijing 100084, China, and College of Mathematics and Computational Science and Guangdong Province Key Laboratory of Computational Science, Sun Yat-sen University, Guangzhou 510275, China (ziye101@163.com).
‡Beijing Computational Science Research Center, Beijing 100084, China, and Department of Mathematics, Wayne State University, Detroit, MI 48202 (zzhang@math.wayne.edu). The research of this author is supported in part by the National Natural Science Foundation of China (NSFC) under Grants No. 11471031, No. 91430216, and the US National Science Foundation (NSF) through grants DMS-1115530 and DMS-1419040.
§College of Mathematics and Computational Science and Guangdong Province Key Laboratory of Computational Science, Sun Yat-sen University, Guangzhou 510275, China (mcszgs@mail.sysu.edn.cn). The research of this author was supported in part by the National Natural Science Foundation of China under grant 11171359.

of this remarkable property remains open. Indeed, the $2k+1$th superconvergence rate is one of the unsolved mysteries of the DG method for hyperbolic equations.

The main purpose of our current work is to address this mystery by offering a rigorous mathematical proof for the $2k+1$th (or $2k+1/2$th) superconvergence rate at downwind points and for the domain average. As by-products, we provide a simplified proof for the pointwise $k+2$th superconvergence rate at the right Radau points, a fact established in [19] in a weaker sense (under a discrete L^2-norm) by a different approach; we also prove a pointwise $k+1$th derivative superconvergence rate at the left Radau points, a fact not established before. By doing so, we present a full picture for superconvergence properties of the DG method for linear hyperbolic equations in one spatial dimension.

To prove the $2k+1$th superconvergence rate, we revisit the problem considered in [19] and make the same assumption that the time integration is exact. The novelty lies in that we adopt a completely different analysis track. An essential ingredient is the design of a correction function w. The idea is motivated from its successful applications to FEMs and finite volume methods (FVMs) for elliptic equations (see, e.g., [5, 6]). However, as the correction function is very different from FVM to FEM, it is much more so for the DG method due to special features of hyperbolic equations different from those of elliptic equations, especially the time-dependent feature. Our approach here is to correct the error between the exact solution u and its truncated Radau expansion P_h^-u (defined in section 3), which interpolates u at all downwind points. With help of the correction function w, which is zero at all downwind points, we prove that the DG solution is superclose (with order $2k+1$) to P_h^-u-w. It is this supercloseness that leads to the $2k+1$th superconvergence rate at the downwind points (in average sense) and for the domain average. As a direct consequence, we obtain another new theoretical result: the derivative approximation of the DG solution is superconvergent at all interior left Radau points with a rate $k+1$. To end this introduction, we would like to point out that all superconvergent results here are valid for one-dimensional linear systems, and the proof is along the same line without any difficulty.

The rest of the paper is organized as follows. In section 2, we present DG schemes for linear conservation laws. Section 3 is the most technical part, where we construct a special interpolation function superclose to the DG solution. Section 4 is the main body of the paper, where superconvergence results are proved with suitable initial discretization. In section 5, we provide some numerical examples to support our theoretical findings. Finally, some possible future works and concluding remarks are presented in section 6.

Throughout this paper, we adopt standard notation for Sobolev spaces such as $W^{m,p}(D)$ on subdomain $D\subset\Omega$ equipped with the norm $\|\cdot\|_{m,p,D}$ and seminorm $|\cdot|_{m,p,D}$. When $D=\Omega$, we omit the index D, and if $p=2$, we set $W^{m,p}(D)=H^m(D)$, $\|\cdot\|_{m,p,D}=\|\cdot\|_{m,D}$, and $|\cdot|_{m,p,D}=|\cdot|_{m,D}$. Notation $A\lesssim B$ implies that A can be bounded by B multiplied by a constant independent of the mesh size h. $A\sim B$ stands for $A\lesssim B$ and $B\lesssim A$.

2. DG schemes. We consider the DG method for the following one-dimensional linear hyperbolic conservation laws:

$$\begin{aligned} &u_t+u_x=0, && (x,t)\in[0,2\pi]\times(0,T],\\ &u(x,0)=u_0(x), && x\in R, \end{aligned} \tag{2.1}$$

where u_0 is sufficiently smooth. We will consider both the periodic boundary condition $u(0,t) = u(2\pi, t)$ and the Dirichlet boundary condition $u(0,t) = g(t)$.

Let $\Omega = [0, 2\pi]$ and $0 = x_{\frac{1}{2}} < x_{\frac{3}{2}} < \cdots < x_{N+\frac{1}{2}}$ be $N+1$ distinct points on the interval Ω. For all positive integers r, we define $\mathbb{Z}_r = \{1, \ldots, r\}$ and denote by

$$\tau_j = (x_{j-\frac{1}{2}}, x_{j+\frac{1}{2}}), \quad x_j = \frac{1}{2}(x_{j-\frac{1}{2}} + x_{j+\frac{1}{2}}),\ j \in \mathbb{Z}_N,$$

the cells and cell centers, respectively. Let $h_j = x_{j+\frac{1}{2}} - x_{j-\frac{1}{2}}$, $\overline{h}_j = h_j/2$, and $h = \max_j h_j$. We assume that the mesh is quasi-uniform, i.e., there exists a constant c such that

$$h \le c h_j, j \in \mathbb{Z}_N.$$

Define

$$V_h = \{v:\ v|_{\tau_j} \in \mathbb{P}_k(\tau_j),\ j \in \mathbb{Z}_N\}$$

to be the finite element space, where $\mathbb{P}_k$ denotes the space of polynomials of degree at most k with coefficients as functions of t. The DG scheme for (2.1) reads as follows: Find $u_h \in V_h$ such that for any $v \in V_h$

$$(u_{ht}, v)_j - (u_h, v_x)_j + \hat{u}_h|_{j+\frac{1}{2}} v^-_{j+\frac{1}{2}} - \hat{u}_h|_{j-\frac{1}{2}} v^+_{j-\frac{1}{2}} = 0, \tag{2.2}$$

where $(u_{ht}, v)_j = \int_{\tau_j} u_{ht} v dx$, $v^-_{j+\frac{1}{2}}$, and $v^+_{j+\frac{1}{2}}$ denote the left and right limits of v at the point $x_{j+\frac{1}{2}}$, respectively, and $\hat{u}_h$ is the numerical flux. In this paper, we consider the upwind flux

$$\hat{u}_h|_{j+\frac{1}{2}} = u_h(x^-_{j+\frac{1}{2}}),\ j \in \mathbb{Z}_N.$$

The numerical flux $\hat{u}_h$ at the boundary $x = x_{\frac{1}{2}}$ is taken as

$$\hat{u}_h|_{\frac{1}{2}} = u_h(x^-_{N+\frac{1}{2}})$$

for the periodic boundary condition and

$$\hat{u}_h|_{\frac{1}{2}} = g$$

for the Dirichlet boundary condition. For simplicity, we still use the notation $\hat{u}_h|_{\frac{1}{2}} = u_h(x^-_{\frac{1}{2}})$.

Define

$$H^1_h = \{v:\ v|_{\tau_j} \in H^1(\tau_j),\ j \in \mathbb{Z}_N\}$$

and for all $w, v \in H^1_h$, let the bilinear form

$$a(w, v) = \sum_{j=1}^{N} a_j(w, v),$$

where

$$a_j(w, v) = (w_t, v)_j - (w, v_x)_j + w^-_{j+\frac{1}{2}} v^-_{j+\frac{1}{2}} - w^-_{j-\frac{1}{2}} v^+_{j-\frac{1}{2}}.$$

Then it is straightforward to deduce from (2.2)

$$a(u_h, v) = 0, \quad v \in V_h.$$

Obviously, the exact solution u also satisfies

$$a(u, v) = 0, \quad v \in V_h.$$

Moreover, if $v \in H_h^1$ satisfies $v_{\frac{1}{2}}^- = 0$ or $v_{\frac{1}{2}}^- = v_{N+\frac{1}{2}}^-$, we have

$$\begin{aligned} a(v,v) &= (v_t, v) + \frac{1}{2}\sum_{j=1}^{N}\left(v_{j+\frac{1}{2}}^- v_{j+\frac{1}{2}}^- + v_{j-\frac{1}{2}}^+ v_{j-\frac{1}{2}}^+ - 2v_{j-\frac{1}{2}}^- v_{j-\frac{1}{2}}^+\right) \\ &= (v_t, v) + \frac{1}{2}\sum_{j=1}^{N}[v]_{j-\frac{1}{2}}^2 + \frac{1}{2}(v_{N+\frac{1}{2}}^- v_{N+\frac{1}{2}}^- - v_{\frac{1}{2}}^- v_{\frac{1}{2}}^-) \\ &\geq (v_t, v), \end{aligned}$$

where $[v]_{j-\frac{1}{2}} = v_{j-\frac{1}{2}}^+ - v_{j-\frac{1}{2}}^-$ denotes the jump of v across $x_{j-\frac{1}{2}}$. Then in both cases,

$$\frac{1}{2}\frac{d}{dt}\|v\|_0^2 = (v_t, v) \leq a(v, v). \tag{2.3}$$

To end this section, we would like to define the Gauss–Radau projection $P_h^- u \in V_h$ of u by

$$(P_h^- u, v)_j = (u, v)_j \quad \forall v \in \mathbb{P}_{k-1}(\tau_j) \quad \text{and} \quad P_h^- u(x_{j+\frac{1}{2}}^-) = u(x_{j+\frac{1}{2}}^-). \tag{2.4}$$

Notice that this special projection is used in the error estimates of the DG methods, e.g., in [8, 19].

3. Construction of a special interpolation function. By (2.3), the estimate for $\|u_h - P_h^- u\|_0$ can usually be reduced to estimating

$$a(u_h - P_h^- u, u_h - P_h^- u) = a(u - P_h^- u, u_h - P_h^- u).$$

A straightforward analysis using the definition of $a(\cdot,\cdot)$ results in

$$\left|a(u - P_h^- u, v)\right| = \left|(u_t - P_h^- u_t, v)\right| \lesssim h^{k+1} \quad \forall v \in V_h,$$

due to the restriction of optimal error bound

$$\|u_t - P_h^- u_t\|_0 \lesssim h^{k+1}.$$

This rate is far from our superconvergence need. To obtain desired superconvergence results, we shall construct in this section a correction function $w \in V_h$ to improve the error between u and $P_h^- u$ such that

$$\left|a(u - P_h^- u + w, v)\right| \lesssim h^{k+1+l}, \quad v \in V_h,$$

for some $l \geq 1$. Our ultimate goal is to have $l = k$. To see the feasibility of this k-order gain, we may count degrees of freedom of w in each element τ_j. We have totally k undetermined coefficients for w (due to a constrain at the right end $x_{j+\frac{1}{2}}^-$), which matches the k-order gain. With the help of w, we are able to show that the DG solution u_h is superclose to the special interpolation function $u_I = P_h^- u - w$. It is this supercloseness that leads to the proof of superconvergence properties of u_h at some special points.

The rest of this section is dedicated to constructing the special interpolation function u_I, or the correction function w. To this end, we begin with some preliminaries.

First, suppose $u(x,t)$ has the following Radau expansion in each element $\tau_j, j \in \mathbb{Z}_N$:

$$u(x,t) = u(x_{j+\frac{1}{2}}^-, t) + \sum_{m=1}^{\infty} u_{j,m}(t)(L_{j,m} - L_{j,m-1})(x), \tag{3.1}$$

where $L_{j,m}, j \in \mathbb{Z}_N, m \geq 1$, is the classic Legendre polynomial of degree m in the interval τ_j and the coefficient

$$u_{j,m}(t) = u(x_{j+\frac{1}{2}}^-, t) - \frac{1}{h_j}\int_{\tau_j} u(x,t) \sum_{l=0}^{m-1}(2l+1)L_{j,l}(x)dx. \tag{3.2}$$

By the definition of $P_h^- u$ in (2.4), we obtain

$$(P_h^- u)(x,t) = u(x_{j+\frac{1}{2}}^-, t) + \sum_{m=1}^{k} u_{j,m}(t)(L_{j,m} - L_{j,m-1})(x), \tag{3.3}$$

which yields

$$a_j(u - P_h^- u, v) = (u_t - P_h^- u_t, v)_j = -\partial_t u_{j,k+1}(L_{j,k}, v)_j \quad \forall v \in V_h, \tag{3.4}$$

where $u_{j,k+1}$ is the same as in (3.2). Note that $u = P_h^- u$ when $u \in \mathbb{P}_k$, then $u_{j,k+1} = 0$. By the Bramble–Hilbert lemma, we obtain

$$|u_{j,k+1}| \lesssim h_j^{k+1} \|\partial_x^{k+1} u\|_{0,\infty,\tau_j}. \tag{3.5}$$

Second, for all $v \in H_h^1$, let its average primal function in τ_j be

$$D_s^{-1} v(x) = \frac{1}{\overline{h}_j}\int_{x_{j-\frac{1}{2}}}^{x} v(x')dx' = \int_{-1}^{s} \hat{v}(s')ds', \quad x \in \tau_j, \tag{3.6}$$

where

$$s = (x - x_j)/\overline{h}_j \in [-1,1], \quad \hat{v}(s) = v(x).$$

In each element $\tau_j, j \in \mathbb{Z}_N$, we define

$$F_1 = P_h^- D_s^{-1} L_{j,k}, \quad F_i = -P_h^- D_s^{-1} F_{i-1} = -(-P_h^- D_s^{-1})^i L_{j,k}, \ i \geq 2. \tag{3.7}$$

LEMMA 3.1. *For all $1 \leq i \leq k$, F_i has the representation*

$$F_i(x) = \sum_{m=k-i+1}^{k} b_{i,m}(L_{j,m} - L_{j,m-1})(x), x \in \tau_j, \tag{3.8}$$

where the coefficients $b_{i,m}$ *are independent of the mesh size* h_j. *Consequently,*

$$F_i(x^-_{j+\frac{1}{2}}) = 0, \quad \|F_i\|_{0,\infty,\tau_j} \lesssim 1, \tag{3.9}$$

$$(F_i, v)_j = 0 \quad \forall v \in \mathbb{P}_{k-i-1}(\tau_j). \tag{3.10}$$

Proof. We will show (3.8) by induction. First, a straightforward calculation yields

$$D_s^{-1} L_{j,k} = \frac{1}{2k+1}(L_{j,k+1} - L_{j,k-1}),$$

and thus

$$F_1 = \frac{1}{2k+1}(L_{j,k} - L_{j,k-1}),$$

which implies (3.8) is valid for $i = 1$ with $b_{1,k} = \frac{1}{2k+1}$.

Now we suppose $F_i, i \le k-1$, has the representation (3.8). Since for all $m \ge 1$,

$$D_s^{-1} L_{j,m} = \frac{1}{2m+1}(L_{j,m+1} - L_{j,m-1})$$

and

$$P_h^- L_{j,k+1} = L_{j,k}, \quad P_h^- L_{j,m} = L_{j,m}, \quad m \le k,$$

it is easy to deduce that

$$F_{i+1} = -P_h^- D_s^{-1} F_i = \sum_{m=k-i}^{k} b_{i+1,m}(L_{j,m} - L_{j,m-1})$$

with

$$\begin{aligned} b_{i+1,k-i} &= \frac{b_{i,k-i+1}}{2(k-i)+1}, \\ b_{i+1,k-i+1} &= \frac{b_{i,k-i+2}}{2(k-i)+3} - \frac{b_{i,k-i+1}}{2(k-i)+3} + \frac{b_{i,k-i+1}}{2(k-i)+1}, \\ b_{i+1,k} &= -\frac{b_{i,k-1}}{2k-1} - \frac{b_{i,k}}{2k+1} + \frac{b_{i,k}}{2k-1}, \end{aligned}$$

and for all $m = k-i+2, \dots, k-1$,

$$b_{i+1,m} = \frac{b_{i,m+1} - b_{i,m}}{2m+1} + \frac{b_{i,m} - b_{i,m-1}}{2m-1}.$$

Therefore (3.8) is valid for $i+1$. Consequently, (3.8) is valid for all $1 \le i \le k$.

Since $L_{j,m}(x^-_{j+\frac{1}{2}}) = 1$ for all $m \ge 1$, the first formula of (3.9) holds. Moreover, by the iterative relations between the coefficients of $b_{i,m}, 1 \le i \le k, k-i+1 \le m \le k$, we have $|b_{i,m}| \lesssim 1$, the second formula of (3.9) follows from the fact that $\|L_{j,m}\|_{0,\infty,\tau_j} = 1$. Finally, by the orthogonality of the Legendre polynomials, the formula (3.10) is valid. ∎

With all the preparations, we are now ready to construct our correction function w^l for some l, where $1 \le l \le k$. We define, at the boundary point $x = x_{\frac{1}{2}} = 0$,

$$w^l(x^-_{\frac{1}{2}}, t) = 0 \ \ \forall t \ge 0,$$

and in each element $\tau_j, j \in \mathbb{Z}_N$,

$$w^l(x,t) = \sum_{i=1}^{l} w_i(x,t), \quad w_i(x,t) = (\overline{h}_j)^i G_i(t) F_i(x) \tag{3.11}$$

with

$$G_i(t) = \partial_t^i u_{j,k+1}(t). \tag{3.12}$$

By the first formula in (3.9), $F_i(x^-_{j+\frac{1}{2}}) = 0$; then $w_i(x^-_{j+\frac{1}{2}}, t) = 0$ for all $i \ge 0$. Then

$$w^l(x^-_{j+\frac{1}{2}}, t) = 0 \quad \forall t \ge 0, j \in \mathbb{Z}_N. \tag{3.13}$$

In the following, we define the special interpolation function

$$u_I^l = P_h^- u - w^l \tag{3.14}$$

and discuss the properties of $a_j(u - u_I^l, v)$.

THEOREM 3.2. *Let $u_I^l \in V_h$ be defined by* (3.14), (3.11), (3.12), *and* (3.7) *with $1 \le l \le k$. Then if $u \in W^{k+l+2,\infty}(\Omega), k \ge 1$, we have*

$$|a_j(u - u_I^l, v)| \lesssim h^{k+l+1} \|u\|_{k+l+2,\infty,\tau_j} \|v\|_{0,1,\tau_j} \quad \forall v \in V_h. \tag{3.15}$$

Proof. By the definition of $a_j(\cdot,\cdot)$ and the fact that $w_i(x^-_{j-\frac{1}{2}}, t) = w_i(x^-_{j+\frac{1}{2}}, t) = 0$,

$$a_j(w_i, v) = (w_{it}, v)_j - (w_i, v_x)_j.$$

For all $1 \le i \le l-1 < k$, recalling the definition of w_i in (3.11), we have, from integration by parts and the fact that $D_s^{-1} F_i(x^-_{j+\frac{1}{2}}) = D_s^{-1} F_i(x^+_{j-\frac{1}{2}}) = 0$,

$$\begin{aligned} (w_{it}, v)_j &= (\overline{h}_j)^i G_{i+1} (F_i, v)_j \\ &= -(\overline{h}_j)^{i+1} G_{i+1} (D_s^{-1} F_i, v_x)_j \\ &= (\overline{h}_j)^{i+1} G_{i+1} (F_{i+1}, v_x)_j \\ &= (w_{i+1}, v_x)_j. \end{aligned}$$

Then

$$a_j(w_i, v) = (w_{i+1} - w_i, v_x)_j, \quad 1 \le i \le l-1,$$

and thus

$$a_j(w^l, v) = \sum_{i=1}^{l} a_j(w_i, v) = (w_{lt}, v)_j - (w_1, v_x)_j.$$

By (3.4), $a_j(u - P_h^- u, v) = (w_1, v_x)_j$. Then

$$a_j(u - u_I^l, v) = a_j(u - P_h^- u + w^l, v) = (w_{lt}, v)_j = (\overline{h}_j)^l G_{l+1} (F_l, v)_j. \tag{3.16}$$

Consequently,

$$\begin{aligned} |a_j(u - u_I^l, v)| &\lesssim h_j^l \|v\|_{0,1,\tau_j} |G_{l+1}| \\ &\lesssim h_j^{k+l+1} \|u\|_{k+l+2,\infty,\tau_j} \|v\|_{0,1,\tau_j}, \end{aligned}$$

where in the last inequality, we have used (3.5) and the fact that

$$|G_{l+1}| = |\partial_t^{l+1} u_{j,k+1}| \lesssim h_j^{k+1} \|\partial_x^{k+1}\partial_t^{l+1} u\|_{0,\infty,\tau_j}.$$

The proof is completed. ∎

Remark 3.3. As a direct consequence of (3.15),

$$\left|a(u - u_I^l, v)\right| \lesssim h^{k+l+1}\|u\|_{k+l+2,\infty}\|v\|_{0,1}. \tag{3.17}$$

4. Superconvergence. In this section, we shall study superconvergence properties of the DG solution, including superconvergence for the domain average and at some special points: downwind points ($x^-_{j+1/2}$), left and right Radau points of degree $k+1$ on each τ_j, which can be obtained by linear mapping from the left and right Radau points of degree $k+1$ on the interval $[-1,1]$, and the latter are zeros of the left Radau polynomial $L_{k+1}+L_k$ and the right Radau polynomial $L_{k+1}-L_k$, respectively. Here L_m denotes the Legendre polynomial of degree m in the interval $[-1,1]$.

We begin with a study of the difference between the interpolation function $u_I^l = P_h^- u - w^l$ and the DG solution u_h.

THEOREM 4.1. *Let $u \in W^{k+l+2,\infty}(\Omega), u_h \in V_h$ be the solution of* (2.1) *and* (2.2)*, respectively. Suppose $u_I^l \in V_h$ is defined by* (3.14), (3.11), (3.12)*, and* (3.7)*. Then for both Dirichlet and periodic boundary conditions,*

$$\|u_I^l - u_h\|_0(t) \lesssim \|u_I^l - u_h\|_0(0) + th^{k+l+1}\|u\|_{k+l+2,\infty}. \tag{4.1}$$

Proof. Since

$$(u_I^l - u_h)^-_{N+\frac{1}{2}} = (u_I^l - u_h)^-_{\frac{1}{2}}$$

for the periodic boundary condition and

$$(u_I^l - u_h)^-_{\frac{1}{2}} = 0$$

for the Dirichlet boundary condition, (2.3) is valid for both cases if we choose $v = u_I^l - u_h$. Noticing (3.17), we have

$$\begin{aligned}\|u_I^l - u_h\|_0 \frac{d}{dt}\|u_I^l - u_h\|_0 &\le \left|a(u_h - u_I^l, u_I^l - u_h)\right| \\ &= \left|a(u - u_I^l, u_I^l - u_h)\right| \\ &\lesssim h^{k+l+1}\|u\|_{k+l+2,\infty}\|u_I^l - u_h\|_0.\end{aligned}$$

Then

$$\frac{d}{dt}\|u_I^l - u_h\|_0 \lesssim h^{k+l+1}\|u\|_{k+l+2,\infty}$$

and (4.1) follows. ∎

Remark 4.2. From Theorem 4.1, we know that the suitable choice of the initial solution is of great importance. To achieve the superconvergence rate $k+l+1$ for $\|u_I^l - u_h\|_0$, the initial error should reach the same convergence rate, that is,

$$\|u_h(\cdot,0) - u_I^l(\cdot,0)\|_0 \lesssim h^{k+l+1}\|u\|_{k+l+2,\infty}. \tag{4.2}$$

We shall demonstrate this point in our numerical analysis. To obtain (4.2), a natural way of initial discretization is to choose

$$u_h(x,0) = u_I^l(x,0) \quad \forall x \in \Omega. \tag{4.3}$$

4.1. Superconvergence at the downwind points. We are now ready to present our superconvergence results of a DG solution at the downwind points.

THEOREM 4.3. *Let $u \in W^{2k+2,\infty}(\Omega)$ be the solution of (2.1) and u_h be the solution of (2.2) with initial value $u_h(\cdot,0)$ chosen such that (4.2) holds with $l = k$. Then for both Dirichlet and periodic boundary conditions,*

$$|(u-u_h)(x^-_{j+\frac{1}{2}},t)| \lesssim (1+t)h^{2k+\frac{1}{2}}\|u\|_{2k+2,\infty} \quad \forall j \in \mathbb{Z}_N \tag{4.4}$$

and

$$\left(\frac{1}{N}\sum_{j=1}^{N}\left(u-u_h\right)^2\left(x^-_{j+\frac{1}{2}},t\right)\right)^{\frac{1}{2}} \lesssim (1+t)h^{2k+1}\|u\|_{2k+2,\infty}. \tag{4.5}$$

Moreover, if we choose the initial value $u_h(\cdot,0) = u_I^k(\cdot,0)$, we have the following improved results:

$$|(u-u_h)(x^-_{j+\frac{1}{2}},t)| \lesssim th^{2k+\frac{1}{2}}\|u\|_{2k+2,\infty} \quad \forall j \in \mathbb{Z}_N \tag{4.6}$$

and

$$\left(\frac{1}{N}\sum_{j=1}^{N}\left(u-u_h\right)^2\left(x^-_{j+\frac{1}{2}},t\right)\right)^{\frac{1}{2}} \lesssim th^{2k+1}\|u\|_{2k+2,\infty}. \tag{4.7}$$

Proof. If $u_h(\cdot,0)$ satisfies (4.2) with $l = k$, we have from (4.1)

$$\|u_I - u_h\|_0(t) \lesssim (1+t)h^{2k+1}\|u\|_{2k+2,\infty}, \tag{4.8}$$

where $u_I = u_I^k$. For any fixed t, $u_I - u_h \in \mathbb{P}_k$ in each $\tau_j, j \in \mathbb{Z}_N$. Then the inverse inequality holds and thus

$$\begin{aligned}\left|(u_I-u_h)(x^-_{j+\frac{1}{2}},t)\right| &\le \|u_I-u_h\|_{0,\infty,\tau_j}(t)\\ &\lesssim h^{-\frac{1}{2}}\|u_I-u_h\|_{0,\tau_j}(t)\\ &\lesssim (1+t)h^{2k+\frac{1}{2}}\|u\|_{2k+2,\infty}.\end{aligned}$$

By the fact that $u(x^-_{j+\frac{1}{2}}) = P_h^- u(x^-_{j+\frac{1}{2}})$ and $w^k(x^-_{j+\frac{1}{2}}) = 0$, we have

$$u_I(x^-_{j+\frac{1}{2}}) = u(x^-_{j+\frac{1}{2}}) \quad \forall j \in \mathbb{Z}_N.$$

Then the desired result (4.4) follows.

We next show (4.5). Again by the inverse inequality,

$$\sum_{j=1}^{N}\|u_I-u_h\|^2_{0,\infty,\tau_j} \lesssim \sum_{j=1}^{N}h_j^{-1}\|u_I-u_h\|^2_{0,\tau_j} \lesssim N\|u_I-u_h\|_0^2.$$

Then

$$\frac{1}{N}\sum_{j=1}^{N}\left(u-u_h\right)^2(x^-_{j+\frac12},t) = \frac{1}{N}\sum_{j=1}^{N}\left(u_I-u_h\right)^2(x^-_{j+\frac12},t)$$
$$\leq \frac{1}{N}\sum_{j=1}^{N}\|u_I-u_h\|^2_{0,\infty,\tau_j}(t)$$
$$\lesssim \|u_I-u_h\|_0^2(t).$$

The inequality (4.5) follows directly from the estimate (4.8).

If the initial value $u_h(\cdot,0)=u_I(\cdot,0)$, then

$$\|u_I-u_h\|_0(t)=\int_0^t \frac{d}{dt}\|u_I-u_h\|_0(s)ds \lesssim th^{2k+1}\|u\|_{2k+2,\infty}.$$

Following the same line, we obtain (4.6) and (4.7) directly. ∎

Remark 4.4. By (4.8), the interpolation function u_I is superclose to the DG solution u_h with the superconvergence rate $2k+1$.

4.2. Superconvegence for the domain average. We have the following superconvergence results for the domain average of $u-u_h$.

THEOREM 4.5. *Let $u\in W^{2k+2,\infty}(\Omega)$ be the solution of* (2.1) *and u_h be the solution of* (2.2)*. Suppose the initial solution $u_h(\cdot,0)=P_h^-u(\cdot,0)-w^k(\cdot,0)$ with w^k defined by* (3.11)*. Then*

$$\left|\frac{1}{2\pi}\int_0^{2\pi}(u-u_h)(x,t)dx\right| \lesssim (h^{\frac12}+t^2)h^{2k+\frac12}\|u\|_{2k+2,\infty} \tag{4.9}$$

for the Dirichlet boundary condition and

$$\left|\frac{1}{2\pi}\int_0^{2\pi}(u-u_h)(x,t)dx\right| \lesssim h^{2k+1}\|u\|_{2k+1,\infty} \tag{4.10}$$

for the periodic boundary condition.

Proof. We first estimate the domain average of $u-u_h$ at time $t=0$. Note that

$$\int_0^{2\pi}(u-u_h)(x,0)dx = \int_0^{2\pi}(P_h^-u-u_h)(x,0)dx = \int_0^{2\pi} w^k(x,0)dx.$$

By (3.8), (3.11)–(3.12), we derive

$$\int_{x_{j-\frac12}}^{x_{j+\frac12}} w^k(x,t)dx = \int_{x_{j-\frac12}}^{x_{j+\frac12}} w_k(x,t)dx = (\overline{h}_j)^k G_k \int_{x_{j-\frac12}}^{x_{j+\frac12}} F_k(x)dx \quad \forall j\in\mathbb{Z}_N.$$

Here G_k and F_k are the same as in (3.12) and (3.7), respectively. By the second inequality of (3.9) and the fact that

$$|G_k| \lesssim h_j^{k+1}\|\partial_t^k\partial_x^{k+1}u\|_{0,\infty,\tau_j} \lesssim h_j^{k+1}\|u\|_{2k+1,\infty,\tau_j},$$

we have

$$\left|\int_{x_{j-\frac12}}^{x_{j+\frac12}} w^k(x,t)dx\right| \lesssim h^{2k+2}\|u\|_{2k+1,\infty,\tau_j},$$

which yields

$$\left|\int_0^{2\pi} w^k(x,t)dx\right| = \left|\sum_{j=1}^{N}\int_{x_{j-\frac{1}{2}}}^{x_{j+\frac{1}{2}}} w^k(x,t)dx\right| \lesssim h^{2k+1}\|u\|_{2k+1,\infty}.$$

Thus,

$$\left|\int_0^{2\pi}(u-u_h)(x,0)dx\right| \lesssim h^{2k+1}\|u\|_{2k+1,\infty}.$$

On the other hand, taking $v=1$ in (2.2) and summing up all j, we obtain

$$\begin{aligned}\int_0^{2\pi}(u-u_h)_t(x,t)dx &= \sum_{j=1}^{N}(u-u_h)^-_{j+\frac{1}{2}}(t)-(u-u_h)^-_{j-\frac{1}{2}}(t)\\ &= (u-u_h)^-_{N+\frac{1}{2}}(t)-(u-u_h)^-_{\frac{1}{2}}(t).\end{aligned}$$

Then for the periodic boundary condition,

$$\frac{d}{dt}\int_0^{2\pi}(u-u_h)(x,t)dx = \int_0^{2\pi}(u-u_h)_t(x,t)dx = 0,$$

and for the Dirichlet boundary condition,

$$\left|\frac{d}{dt}\int_0^{2\pi}(u-u_h)(x,t)dx\right| = \left|(u-u_h)^-_{N+\frac{1}{2}}(t)\right| \lesssim th^{2k+\frac{1}{2}}\|u\|_{2k+2,\infty},$$

where in the last step we have used (4.6). Note that

$$\int_0^{2\pi}(u-u_h)(x,t)dx = \int_0^{2\pi}(u-u_h)(x,0)dx + \int_0^{t}\frac{d}{dt}\int_0^{2\pi}(u-u_h)(x,t)dxdt.$$

Then the desired results follow. ∎

4.3. Superconvergence at the left Radau points. For all $j\in\mathbb{Z}_N$, we denote by $R_{j,l}$, where $l=0,\dots,k$, the zeros of $L_{j,k+1}+L_{j,k}$, namely, the left Radau points on the interval τ_j. We shall prove that the derivative error of $u-u_h$ is superconvergent at all left Radau points $R_{j,l}$, where $l\in\mathbb{Z}_k$, except the point $R_{j,0}=x_{j-\frac{1}{2}}$.

LEMMA 4.6. *Let $u\in W^{k+2,\infty}(\Omega)$ be the solution of* (2.1). *Then*

$$\left|\partial_x(u-P_h^-u)(R_{j,l},t)\right| \lesssim h^{k+1}\|u\|_{k+2,\infty} \quad \forall t\ge 0, j\in\mathbb{Z}_N, l\in\mathbb{Z}_k. \tag{4.11}$$

Proof. In each element $\tau_j, j\in\mathbb{Z}_N$, we have, from (3.1) and (3.3),

$$\partial_x(u-P_h^-u)(x,t) = \sum_{m=k+1}^{\infty} u_{j,m}(t)\partial_x(L_{j,m}-L_{j,m-1})(x).$$

It is shown in [20] that

$$m(L_m+L_{m-1})(s) = (s+1)\partial_s(L_m-L_{m-1})(s), \quad s\in[-1,1],$$

Then by a scaling from $[-1,1]$ to $[x_{j-\frac{1}{2}}, x_{j+\frac{1}{2}}]$, we obtain

$$\partial_x(u - P_h^- u)(x,t) = (k+1)u_{j,k+1}\frac{(L_{j,k+1}+L_{j,k})(x)}{x - x_{j-\frac{1}{2}}} + \sum_{p=k+2}^{\infty} u_{j,p}\partial_x(L_{j,p} - L_{j,p-1})(x).$$

Note that the first term of the above equation vanishes at all interior left Radau points $R_{j,l}$, where $l \in \mathbb{Z}_k$, which yields

$$\partial_x(u - P_h^- u)(R_{j,l},t) = \sum_{p=k+2}^{\infty} u_{j,p}\partial_x(L_{j,p} - L_{j,p-1})(R_{j,l}), \quad l \in \mathbb{Z}_k.$$

Then the desired result (4.11) follows by the standard approximation theory. ∎

We are ready to show the superconvergence results of u_h at the interior left Radau points.

THEOREM 4.7. *Let $u \in W^{k+4,\infty}(\Omega)$ be the solution of (2.1) and u_h be the solution of (2.2) with initial value $u_h(\cdot,0)$ chosen such that (4.2) holds with $l = 2$. Then for both Dirichlet and periodic boundary conditions,*

$$|\partial_x(u - u_h)(R_{j,l},t)| \lesssim (1+t)h^{k+1}\|u\|_{k+4,\infty}, \quad j \in \mathbb{Z}_N, l \in \mathbb{Z}_k. \tag{4.12}$$

Proof. First, by Theorem 4.1 and the initial value chosen, we have

$$\|u_h - u_I^2\|_0 \lesssim (1+t)h^{k+3}\|u\|_{k+4,\infty}.$$

Noticing $u_I^2 = P_h^- u - w^2$ and

$$\|w^2\|_{0,\infty,\tau_j} \lesssim h^{k+2}\|u\|_{k+3,\infty},$$

we obtain

$$\|u_h - P_h^- u\|_{0,\infty,\tau_j} \lesssim (1+t)h^{k+2}\|u\|_{k+4,\infty}, \quad j \in \mathbb{Z}_N. \tag{4.13}$$

Then by the inverse inequality,

$$|P_h^- u - u_h|_{1,\infty} \lesssim (1+t)h^{k+1}\|u\|_{k+4,\infty}.$$

Consequently,

$$\left|\partial_x(P_h^- u - u_h)(R_{j,l},t)\right| \lesssim (1+t)h^{k+1}\|u\|_{k+4,\infty} \quad \forall j \in \mathbb{Z}_N, l \in \mathbb{Z}_k.$$

Combining the above inequality with (4.11) yields (4.12) directly. ∎

4.4. Superconvergence at the right Radau points. As we mentioned in the introduction, one of the main theoretical results in [19] is the superconvergence rate $k+2$ for the function value error of $u - u_h$ at the right Radau points. A by-product of our analysis here is a different and simpler way to establish this fact.

Denote by $R_{j,l}^r$, where $l = 1, \ldots, k+1$, the $k+1$ right Radau points on the interval $\tau_j, j \in \mathbb{Z}_N$. By the standard approximation theory,

$$\left|(u - P_h^- u)(R_{j,l}^r,t)\right| = \left|\sum_{p=k+2}^{\infty} u_{j,p}(t)(L_{j,p} - L_{j,p-1})(R_{j,l}^r)\right| \lesssim h^{k+2}\|u\|_{k+2,\infty}.$$

On the other hand, if the initial value $u_h(\cdot,0)$ is chosen such that (4.2) holds with $l=2$, then (4.13) holds. Consequently,

$$|(u-u_h)(R^r_{j,l},t)| \lesssim (1+t)h^{k+2}\|u\|_{k+4,\infty} \quad \forall t\in(0,T]. \tag{4.14}$$

Remark 4.8. Similarly, if we choose the initial value $u_h(\cdot,0)=u_I^l(\cdot,0)$ instead of letting $u_h(\cdot,0)$ satisfy (4.2) with $l=2$, then by Theorem 4.1,

$$\|u_h-u_I^2\|_0 \lesssim th^{k+3}\|u\|_{k+4,\infty}.$$

By the same arguments as in Theorem 4.7, the term $1+t$ in the estimates (4.12) and (4.14) can be improved to t.

Remark 4.9. In (2.1), we only consider the case in which the advection velocity equals one, while our proof can be extended to a generic velocity. That is, our analysis remains the same for the equation $u_t+au_x=0$, where a is a constant. For the one-dimensional linear system $\mathbf{u}_t+\mathbf{u}_x=\mathbf{0}$, where $\mathbf{u}=(u_1,\dots,u_m)^T$ is a vector, following the same arguments as in (2.1), we obtain the same superconvergence results for each scalar $u_i, i\in\mathbb{Z}_m$. In other words, all the superconvergence results in this paper are still valid for one-dimensional linear systems.

To end this section, we would like to demonstrate how to calculate $u_I^l(x,0), 1\le l\le k$, only using the information of the initial value u_0. Since $u_t+u_x=0$, we have for all integers $i\ge 1$,

$$\partial_t^i u(x,0)=(-1)^i\partial_x^i u_0(x) \quad \forall x\in\Omega.$$

Therefore, by (3.2), for all $i\ge 1$, we have the derivatives

$$\partial_t^i u_{j,k+1}(0)=(-1)^i\left(\partial_x^i u_0(x^-_{j+\frac{1}{2}})-\frac{1}{h_j}\int_{\tau_j}\partial_x^i u_0(x)\sum_{m=0}^{k}(2m+1)L_{j,m}(x)dx\right). \tag{4.15}$$

Now we divide the process into the following steps:

1. In each element τ_j, calculate $G_i=\partial_t^i u_{j,k+1}(0), i\in\mathbb{Z}_l$, by (4.15).
2. Compute $F_i, i\in\mathbb{Z}_l$, from (3.7).
3. Choose $w_i=(\overline{h}_j)^i F_i G_i$ and $w^l=\sum_{i=1}^{l} w_i$.
4. Figure out $u_I^l(x,0)=P_h^- u_0(x)-w^l(x)$.

5. Numerical results. In this section, we present numerical examples to verify our theoretical findings. In our numerical experiments, we shall measure the maximum and average errors at downwind points, the errors for the domain and cell averages, the maximum derivative error at interior left Radau points, and the function value error at right Radau points, respectively. They are defined by

$$e_1=\max_{j\in\mathbb{Z}_N}\left|(u-u_h)(x^-_{j+\frac{1}{2}},T)\right|,\quad e_2=\left(\frac{1}{N}\sum_{j=1}^{N}\left(u-u_h\right)^2\left(x^-_{j+\frac{1}{2}},T\right)\right)^{\frac{1}{2}},$$

$$e_3=\left|\frac{1}{2\pi}\int_0^{2\pi}(u-u_h)(x,T)dx\right|,\quad e_4=\max_{(j,l)\in\mathbb{Z}_N\times\mathbb{Z}_k}\left|\partial_x(u-u_h)(R_{j,l},T)\right|,$$

$$e_5=\max_{(j,l)\in\mathbb{Z}_N\times\mathbb{Z}_{k+1}}\left|(u-u_h)(R^r_{j,l},T)\right|,\quad e_6=\left(\frac{1}{N}\sum_{j=1}^{N}\left(\frac{1}{h_j}\int_{x_{j-\frac{1}{2}}}^{x_{j+\frac{1}{2}}}(u-u_h)(x,T)dx\right)^2\right)^{\frac{1}{2}}.$$

To show the influence of the initial solution on the convergence rate, we also test four different methods for initial discretization in our experiments:

Method 1: $u_h(x,0) = R_h u(x,0)$.

Method 2: $u_h(x,0) = (P_h^- u)(x,0)$.

Method 3: $u_{ht}(x,0) = (P_h^- u_t)(x,0),\ u_h(x^-_{j+\frac{1}{2}},0) = (P_h^- u)(x^-_{j+\frac{1}{2}},0)$.

Method 4: $u_h(x,0) = u_I^k(x,0)$.

Here $R_h u$ in Method 1 denotes the L^2 projection of u. Note that Method 4 is what we use in our superconvergence analysis, while Method 3 is a special way of initial discretization proposed by Yang and Shu in [19]. In light of the frequent use of Methods 1 and 2 for initial discretization of DG methods, we also test them in our experiments as comparison groups.

It should be pointed out that the special initialization we use in Method 4 satisfies the initial condition (4.2) with $l = 2, k$, where $k \geq 3$. In fact, it is easy to see that (4.2) is valid for $l = k$. When $l = 2$, we have, from (3.14), (3.11), (3.12), (3.7), and (3.5),

$$\|u_h(x,0) - u_I^2(x,0)\|_0 = \|u_I^k(x,0) - u_I^2(x,0)\|_0 = \sum_{i=3}^{k} \|w_i\|_0 \lesssim h^{k+3}\|u\|_{k+4,\infty}.$$

In other words, the initialization $u_h(x,0) = u_I^k(x,0)$ in Method 4 satisfies all the initial conditions in Theorems 4.3–4.5 and 4.7.

Example 1. We consider the following equation with the periodic boundary condition:

$$\begin{aligned} &u_t + u_x = 0, \qquad\qquad (x,t) \in [0, 2\pi] \times (0, 3\pi/4], \\ &u(x,0) = e^{\sin(x)}, \\ &u(0,t) = u(2\pi, t). \end{aligned}$$

The exact solution to this problem is

$$u(x,t) = e^{\sin(x-t)}.$$

The problem is solved by the DG scheme (2.2) with $k = 3, 4$, respectively. Piecewise uniform meshes are used in our experiments, which are constructed by equally dividing each interval, $[0, \frac{\pi}{2}]$ and $[\frac{\pi}{2}, 2\pi]$, into $N/2$ subintervals, $N = 4, \ldots, 512$. The ninth order strong-stability preserving Runge–Kutta method [15] with time step $\triangle t = 0.05 h_{min}, h_{min} = \pi/N$ is used to reduce the time discretization error.

Listed in Tables 1–3 are numerical data for errors $e_i, i = 2, \ldots, 6$, and corresponding convergence rates in cases $k = 3, 4$, with the initial solution obtained by Method 4. Depicted in Figure 1 are corresponding error curves with log-log scale.

We observe from Tables 1–3 and Figure 1 a convergence rate $k+1$ for e_4, $k+2$ for e_5, and $2k+1$ for e_2 and e_3, respectively. These results confirm our theoretical findings in Theorems 4.3–4.7 and (4.14): The derivative error is superconvergent at all interior left Radau points and the function value error is superconvergent at all right Radau points, and the average error at downwind points is supercovergent as well as the error for the domain average, with a convergence rate $2k+1$. Moreover, we also observe numerically a $2k+1$ superconvergence rate for the cell average e_6. Our numerical results demonstrate that the superconvergence rates we proved in (4.7), (4.10), (4.12), and (4.14) are optimal.

TABLE 1
Errors $e_i, i = 2, 3, 4,$ and corresponding convergence rates in case $k = 3$.

N	e_2	Rate	e_3	Rate	e_4	Rate
4	2.45e-02	–	5.33e-03	–	1.10e-01	–
8	8.22e-04	5.90	4.64e-05	6.84	1.90e-02	2.40
16	1.04e-05	6.30	2.57e-07	7.50	1.08e-03	4.13
32	8.32e-08	6.96	1.83e-09	7.13	8.42e-05	3.68
64	6.73e-10	6.95	1.39e-11	7.03	5.34e-06	3.98
128	5.32e-12	6.98	1.08e-13	7.01	3.36e-07	3.99
256	4.17e-14	6.99	8.41e-16	7.00	2.10e-08	4.00
512	3.26e-16	7.00	6.57e-18	7.00	1.31e-09	4.00

TABLE 2
Errors $e_i, i = 2, 3, 4,$ and corresponding convergence rates in case $k = 4$.

N	e_2	Rate	e_3	Rate	e_4	Rate
4	5.48e-03	–	1.37e-03	–	5.53e-02	–
8	5.90e-05	6.53	2.15e-06	9.31	1.39e-03	5.31
16	2.12e-07	8.12	3.03e-09	9.47	9.37e-05	3.89
32	3.77e-10	9.13	4.96e-12	9.26	4.26e-06	4.45
64	7.61e-13	8.95	9.33e-15	9.05	1.47e-07	4.86
128	1.50e-15	8.99	1.81e-17	9.01	4.70e-09	4.97
256	2.94e-18	8.99	3.52e-20	9.00	1.47e-10	4.99
512	5.76e-21	9.00	6.87e-23	9.00	4.62e-12	5.00

TABLE 3
Errors e_5, e_6 and corresponding convergence rates in cases $k = 3, 4$.

N	$k = 3$				$k = 4$			
	e_5	Rate	e_6	Rate	e_5	Rate	e_6	Rate
4	5.39e-02	–	9.35e-03	–	1.34e-02	–	2.19e-03	–
8	3.12e-03	4.11	1.60e-04	5.87	2.15e-04	5.96	1.15e-05	7.57
16	8.99e-05	5.12	6.93e-06	4.53	4.31e-06	5.64	9.43e-08	6.93
32	2.68e-06	5.07	7.88e-08	6.46	9.62e-08	5.49	3.48e-10	8.08
64	8.33e-08	5.01	6.66e-10	6.89	1.65e-09	5.86	7.48e-13	8.86
128	2.59e-09	5.01	5.32e-12	6.97	2.64e-11	5.97	1.50e-15	8.96
256	8.07e-11	5.00	4.18e-14	6.99	4.14e-13	5.99	2.95e-18	9.00
512	2.52e-12	5.00	3.27e-16	7.00	6.47e-15	6.00	5.77e-21	9.00

We also test the superconvergence for the maximum error at downwind points by using the four different methods mentioned above for initial discretization. We list in Tables 4 and 5 the approximation error e_1 and the corresponding convergence rate in cases $k = 3, 4$, respectively. It seems that different choices of the initial solution lead to different convergence rates. We observe that when using Method 4, the convergence rate is of order $2k + 1$, half an order higher than the one given in (4.4). On the other hand, Methods 1–3 do not result in the superconvergence rate $2k + 1$. Therefore, the superconvergence rate of $2k+1$ is very sensitive to the method of initialization. As we point out in Remark 4.2, to achieve the superconvergence rate $2k + 1$ for $\|u_h - u_I^k\|_0$, the initial error should reach the same convergence rate. It is this supercloseness that may lead to the $2k + 1$th superconvergence rate at the downwind points. In conclusion, the manner of initial discretization influences the superconvergence rate at the downwind points.

Example 2. We consider the following problem with the Dirichlet boundary condition:

Table 4
e_1 and corresponding convergence rates for different initial discretizations in case $k = 3$.

N	Method 1		Method 2		Method 3		Method 4	
	e_1	Rate	e_1	Rate	e_1	Rate	e_1	Rate
4	4.09e-02	–	4.33e-02	–	4.37e-02	–	4.51e-02	–
8	2.09e-03	4.29	2.11e-03	4.36	1.95e-03	4.49	2.20e-03	4.36
16	5.63e-05	5.21	3.71e-05	5.83	3.39e-05	5.85	3.32e-05	6.05
32	1.40e-06	5.33	3.75e-07	6.63	3.67e-07	6.53	3.10e-07	6.74
64	5.02e-08	4.80	3.57e-09	6.72	3.46e-09	6.73	2.53e-09	6.94
128	1.97e-09	4.67	6.01e-11	5.89	3.32e-11	6.71	2.00e-11	6.98
256	8.43e-11	4.55	1.06e-12	5.82	3.40e-13	6.61	1.57e-13	6.99
512	3.73e-12	4.50	2.49e-14	5.41	3.77e-15	6.49	1.23e-15	7.00

Table 5
e_1 and corresponding convergence rates for different initial discretizations in case $k = 4$.

N	Method 1		Method 2		Method 3		Method 4	
	e_1	Rate	e_1	Rate	e_1	Rate	e_1	Rate
4	1.05e-02	–	1.06e-02	–	1.03e-02	–	1.09e-02	–
8	2.12e-04	5.63	1.61e-04	6.04	1.61e-04	6.00	1.60e-04	6.09
16	2.27e-06	6.54	8.23e-07	7.61	7.63e-07	7.72	6.19e-07	8.02
32	8.71e-08	4.71	5.25e-09	7.29	2.21e-09	8.43	1.44e-09	8.75
64	1.98e-09	5.46	8.45e-11	5.96	9.46e-12	7.87	2.94e-12	8.94
128	1.67e-11	6.89	1.04e-12	6.35	2.76e-14	8.42	5.82e-15	8.98
256	6.36e-13	4.71	1.17e-14	6.47	1.72e-16	7.32	1.14e-17	9.00
512	1.02e-14	5.96	1.25e-16	6.55	9.06e-19	7.57	2.23e-20	9.00

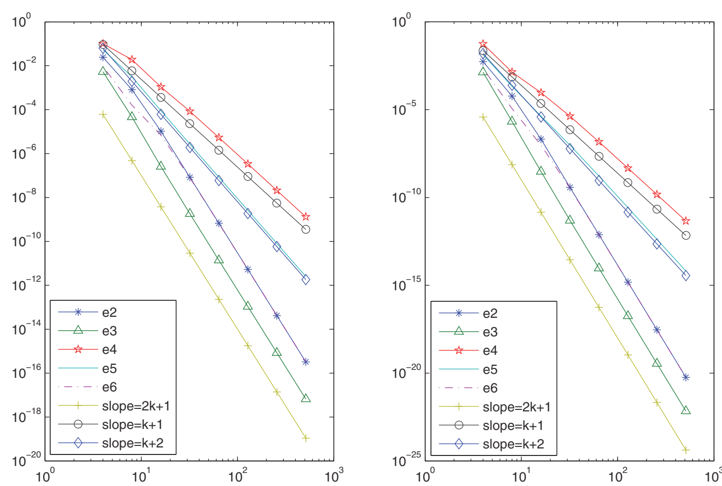

Fig. 1. *Left: $k = 3$; right: $k = 4$.*

$$
\begin{aligned}
&u_t + u_x = 0, \qquad (x,t) \in [0, 2\pi] \times (0, \pi],\\
&u(x,0) = \sin(x),\\
&u(0,t) = -\sin(t).
\end{aligned}
$$

The exact solution to this problem is

$$u(x,t) = \sin(x - t).$$

We construct our meshes by dividing the interval $[0, 2\pi]$ into N subintervals, $N = 2, \ldots, 64$, and solve this problem by the DG scheme (2.2) with polynomial

Table 6
Errors $e_i, i = 2, 3, 4,$ and corresponding convergence rates in case $k = 3$.

N	e_2	Rate	e_3	Rate	e_4	Rate
2	1.83e-03	–	8.64e-04	–	1.01e-02	–
4	2.68e-05	6.10	8.04e-06	6.75	2.14e-03	2.24
8	2.22e-07	6.91	6.56e-08	6.94	1.66e-04	3.68
16	1.78e-09	6.96	5.14e-10	6.99	1.09e-05	3.93
32	1.41e-11	6.98	4.01e-12	7.00	6.90e-07	3.99
64	1.10e-13	6.99	3.12e-14	7.00	4.31e-08	4.00

Table 7
Errors $e_i, i = 2, 3, 4,$ and corresponding convergence rates in case $k = 4$.

N	e_2	Rate	e_3	Rate	e_4	Rate
2	5.00e-05	–	2.77e-05	–	7.08e-03	–
4	2.11e-07	7.89	6.20e-08	8.80	1.85e-04	5.26
8	4.29e-10	8.94	1.25e-10	8.95	7.24e-06	4.68
16	8.56e-13	8.97	2.45e-13	9.00	2.38e-07	4.93
32	1.68e-15	9.00	4.77e-16	9.00	7.55e-09	4.98
64	3.29e-18	8.99	9.29e-19	9.00	2.36e-10	5.00

Table 8
Errors e_5, e_6 and corresponding convergence rates in cases $k = 3, 4$.

N	$k=3$				$k=4$			
	e_5	Rate	e_6	Rate	e_5	Rate	e_6	Rate
2	7.60e-03	–	2.41e-03	–	1.75e-03	–	7.97e-05	–
4	3.96e-04	4.26	2.61e-05	6.53	2.29e-05	6.26	2.05e-07	8.60
8	1.38e-05	4.85	2.41e-07	6.76	4.36e-07	5.71	4.64e-10	8.79
16	4.44e-07	4.95	1.98e-09	6.93	7.14e-09	5.93	9.43e-13	8.94
32	1.40e-08	4.99	1.57e-11	6.98	1.13e-10	5.98	1.86e-15	8.98
64	4.39e-10	5.00	1.23e-13	6.99	1.77e-12	6.00	3.66e-18	8.99

degree $k = 3, 4$, respectively. To diminish the time discretization error, we use the fourth order Runge–Kutta method with time step $\triangle t = T/n$ for $n = 10N^2$ in $k = 3$ and $n = 5N^3$ in $k = 4$.

Numerical data are demonstrated in Tables 6–8, and corresponding error curves are depicted in Figure 2 on the log-log scale with the initial solution obtained by Method 4. Again, we observe a convergence rate $k+1$ for e_4, $k+2$ for e_5, and $2k+1$ for e_2, e_3, and e_6, respectively. These results verify our theoretical findings in Theorems 4.3–4.7 and (4.14). Note that the superconvergence rate $2k+1$ for the domain average is half an order higher than the one given in (4.9).

As in Example 1, we also test convergence rates at the downwind points under the aforementioned four different initial discretization methods. Tables 9 and 10 demonstrate corresponding errors and convergence rates, from which we observe similar results as in the periodic boundary condition: the convergence rate of e_1 is $2k+1$ for Method 4 but not for Methods 1 and 2. As for Method 3, it seems that the superconvergence rate is $2k+1$ for $k = 3$. However, it is not valid for $k = 4$.

6. Conclusion. In this work, we have studied superconvergence properties of the DG method for linear hyperbolic conservation laws in the one-dimensional setting. Our main theoretical result is the proof of the $2k+1$-superconvergence rate at the downwind points in an average sense (Theorem 4.3; (4.5) and (4.7)) as well as for the domain average (Theorem 4.5, (4.10)) and thereby settle a long-standing theoretical conjecture. An unexpected discovery is that in order to achieve the $2k+1$ rate,

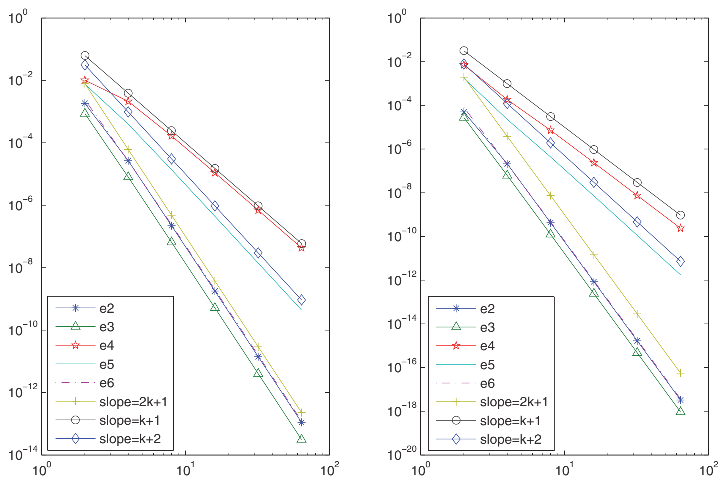

FIG. 2. *Left:* $k = 3$*; right:* $k = 4$.

TABLE 9
e_1 and corresponding convergence rates for different initial discretizations in case $k = 3$.

N	Method 1		Method 2		Method 3		Method 4	
	e_1	Rate	e_1	Rate	e_1	Rate	e_1	Rate
2	8.23e-03	–	4.63e-03	–	4.88e-03	–	1.94e-03	–
4	2.88e-04	4.83	2.23e-05	7.70	5.93e-05	6.36	4.61e-05	5.39
8	1.26e-05	4.51	1.11e-06	4.33	5.21e-07	6.83	3.92e-07	6.88
16	1.81e-07	6.15	1.74e-08	6.00	3.54e-09	7.20	3.16e-09	6.96
32	6.10e-10	8.23	2.94e-10	5.89	2.96e-11	6.90	2.49e-11	6.99
64	1.39e-11	5.44	4.66e-12	5.98	2.32e-13	7.00	1.95e-13	7.00

TABLE 10
e_1 and corresponding convergence rates for different initial discretizations in case $k = 4$.

N	Method 1		Method 2		Method 3		Method 4	
	e_1	Rate	e_1	Rate	e_1	Rate	e_1	Rate
2	1.43e-04	–	8.26e-05	–	1.09e-04	–	5.25e-05	–
4	2.69e-05	2.41	2.02e-06	5.36	1.00e-06	6.77	3.66e-07	7.16
8	7.85e-07	5.10	1.25e-08	7.33	1.10e-08	6.51	7.60e-10	8.91
16	2.02e-08	5.28	9.26e-11	7.08	7.71e-11	7.16	1.51e-12	8.97
32	3.81e-10	5.73	5.13e-12	4.18	3.72e-13	7.70	2.96e-15	8.99
64	4.78e-12	6.31	7.23e-14	6.15	1.52e-15	7.94	5.80e-18	9.00

a proper implementation of the initial solution based on the correction procedure introduced in this paper is crucial for $k > 3$. This observation is supported by a numerical comparison with traditional implementations of the initial solution. Indeed, only Method 4 (based on our correction scheme) can achieve a $2k + 1$ rate for $k = 4$.

As a by-product, we also proved, for the first time, a pointwise derivative superconvergence rate $k + 1$ at all left Radau points (Theorem 4.7, (4.12)). At this point, our proof for the pointwise superconvergence rate $2k + 1/2$ at the downwind points (Theorem 4.3; (4.4) and (4.6)) is still suboptimal (comparing with the numerical rate $2k + 1$). In addition, the proof of $2k + 1$ rate for the cell average remains open. Our other ongoing works include convection-diffusion equations as discussed in [8] and higher dimensional conservation laws.

Finally, we would like to indicate that all aforementioned theoretical results are valid for nonuniform grids since we only assume quasi-uniform meshes in our analysis.

REFERENCES

[1] S. Adjerid, K. D. Devine, J. E. Flaherty, and L. Krivodonova, *A posteriori error estimation for discontinuous Galerkin solutions of hyperbolic problems,* Comput. Methods Appl. Mech. Engrg., 191 (2002), pp. 1097–1112.

[2] S. Adjerid and T. C. Massey, *Superconvergence of discontinuous Galerkin solutions for a nonlinear scalar hyperbolic problem,* Comput. Methods Appl. Mech. Engrg., 195 (2006), pp. 3331–3346.

[3] S. Adjerid and T. Weinhart, *Discontinuous Galerkin error estimation for linear symmetric hyperbolic systems,* Comput. Methods Appl. Mech. Engrg., 198 (2009), 3113–3129.

[4] S. Adjerid and T. Weinhart, *Discontinuous Galerkin error estimation for linear symmetrizable hyperbolic systems,* Math. Comp., 80 (2011), pp. 1335–1367.

[5] W. Cao, Z. Zhang, and Q. Zou, *Is* $2k$*-conjecture valid for finite volume methods?*, arXiv:1401.0372 [math.NA], 2014.

[6] C. Chen and S. Hu, *The highest order superconvergence for bi-*k *degree rectangular elements at nodes: A proof of* $2k$*-conjecture,* Math. Comp., 82 (2013), pp. 1337–1355.

[7] Y. Cheng and C. Shu, *Superconvergence and time evolution of discontinuous Galerkin finite element solutions*, J. Comput. Phys., 227 (2008), pp. 9612–9627.

[8] Y. Cheng and C. Shu, *Superconvergence of discontinuous Galerkin and local discontinuous Galerkin schemes for linear hyperbolic and convection-diffusion equations in one space dimension*, SIAM J. Numer. Anal., 47 (2010), pp. 4044–4072.

[9] B. Cockburn, S. Hou, and C. Shu, *The Runge-Kutta local projection discontinuous Galerkin finite element method for conservation laws,* IV*: The multidimensional case*, Math. Comp., 54 (1990), pp. 545–581.

[10] B. Cockburn, S. Lin, and C. Shu, *TVB Runge-Kutta local projection discontinuous Galerkin finite element method for conservation laws,* III*: One dimensional systems*, J. Comput. Phys., 84 (1989), pp. 90–113.

[11] B. Cockburn and C. Shu, *TVB Runge-Kutta local projection discontinuous Galerkin finite element method for coservation laws,* II*: Genaral framework*, Math. Comp., 52 (1989), pp. 411–435.

[12] B. Cockburn and C. Shu, *The Runge-Kutta local projection* $P1$*-discontinuous Galerkin finite element method for scalar conservation laws*, Math. Model. Number. Anal., 25 (1991), pp. 337–361.

[13] B. Cockburn and C. Shu, *The Runge-Kutta discontinuous Galerkin method for conservation laws,* V*: Multidimensional systems*, J. Comput. Phys., 141 (1998), pp. 199–224.

[14] B. Cockburn and C. Shu, *The local discontinuous Galerkin method for time-dependent convection-diffusion systems*, SIAM J. Numer. Anal., 35 (1998), pp. 2440–2463.

[15] S. Gottlieb, C. Shu, and E. Tadmor, *Strong stability-preserving high-order time discretization methods*, SIAM Rev., 43 (2001), pp. 89–112.

[16] W. Guo, X. Zhong, and J. Qiu, *Superconvergence of discontinuous Galerkin and local discontinuous Galerkin methods: Eigen-structure analysis based on Fourier approach*, J. Comput. Phys., 235 (2013), pp. 458–485.

[17] W. H. Reed and T. R. Hill, *Triangular Mesh for Neutron Transport Equation*, Report LA-UR-73-479, Los Alamos Scientific Laboratory, Los Alamos, NM, 1973.

[18] Z. Xie and Z. Zhang, *Uniform superconvergence analysis of the discontinuous Galerkin method for a singularly perturbed problem in* 1*-*D, Math. Comp., 79 (2010), pp. 35–45.

[19] Y. Yang and C. Shu, *Analysis of optimal supercovergence of discontinuous Galerkin method for linear hyperbolic equations*, SIAM J. Numer. Anal., 50 (2012), pp. 3110–3133.

[20] Z. Zhang, *Superconvergence points of spectral interpolation*, SIAM J. Numer. Anal., 50 (2021), pp. 2966–2985.

[21] Z. Zhang, Z. Xie, and Z. Zhang, *Superconvergence of discontinuous Galerkin methods for convection-diffusion problems*, J. Sci. Comput., 41 (2009), pp. 70–93.